Large Scale Laboratory Element Testing of Geogrid Reinforced Soil

A. Ruiken. RWTH Aachen University, Germany. ruiken@geotechnk.rwth-aachen.de
M. Ziegler. RWTH Aachen University, Germany. ziegler@geotechnk.rwth-aachen.de

ABSTRACT

Large scale triaxial tests to investigate the reinforcing effect of geogrids have been carried out at RWTH Aachen University. Results of unreinforced and reinforced test series show a significant increase of the bearing capacity as well as a reduction of the deformations of the tested samples due to the reinforcement. A confining effect of the reinforcement is clearly identified and explained with a mechanical model. A calculation method, which is based on the mechanical model, was used to draw the stress paths for a series of reinforced tests.
In this paper it is also discussed, how the increased strength of the soil can be considered in design. As a result, shear parameters for the tested composite material have been determined from the results of the triaxial testing.

1. LABORATORY TESTING

1.1 Test set-up

Within the framework of the research program, large triaxial tests with 500 mm diameter and approximately 1100 mm height (Fig. 1) have been carried out. The results presented in this paper are obtained from testing of crushed base course material 0/45 (Fig. 2), which was compacted either to 95% or to 100% proctor density (D_{pr}). The samples have been reinforced with a biaxial polypropylene geogrid made of pre-stretched monolithic flat bars that have been welded together. The strength of the geogrid as stated by the manufacturer was 12 kN/m at 2% strain and 24 kN/m at 5% strain respectively.

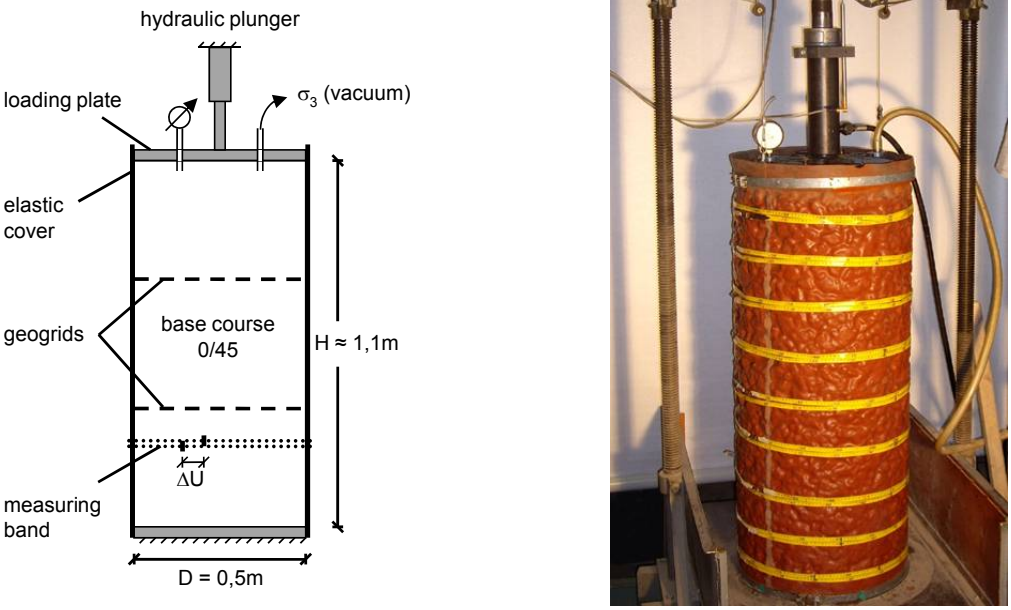

Figure 1. Principal sketch and photograph of large triaxial load cell.

The lateral pressure applied by vacuum was set between 5 kN/m² and 70 kN/m² and kept constant during testing. Three geogrid layers have been placed in the reinforced samples leading to a vertical reinforcement spacing of nearly 0.3 m. During loading of the samples with a strain rate of 0.1%/min, plunger load, average radial strains of the probe and geogrid strains have been recorded. Last mentioned have been recorded with strain gauges glued onto the flat tensile members of the geogrids.

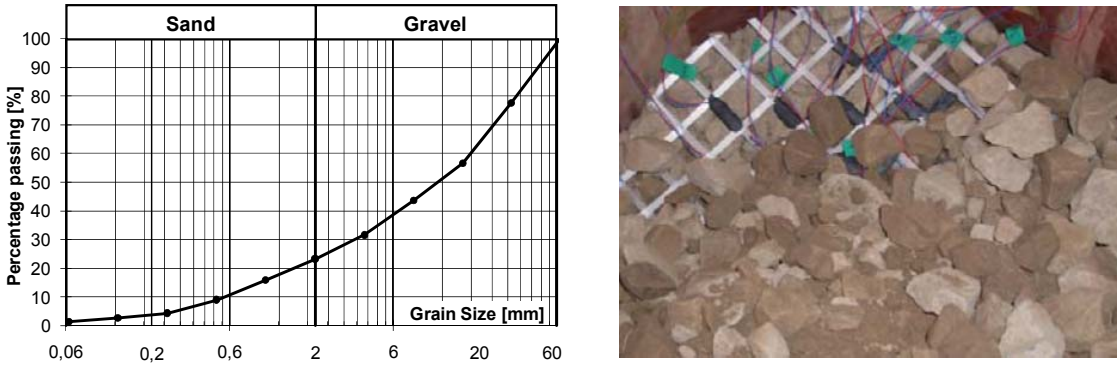

Figure 2. Crushed base course material used in the triaxial tests.

1.2 Test results

Stress-strain curves of tests with unreinforced and reinforced samples compacted to 95% proctor density are given in Fig. 3a for four different confining pressures. The increase of the bearing capacity due to the reinforcements can clearly be seen. However, the initial stiffness of both, unreinforced and reinforced samples seems to be similar for vertical strains up to 0.5% to 1%. This is consistent with the average volumetric strains calculated from the radial and vertical strains, indicating almost pure compaction at the beginning of the tests (Fig. 3b). As soon as the sample starts to extend radially, the geogrids are increasingly activated, which subsequently leads to an increase of the stiffness and the load bearing capacity respectively.

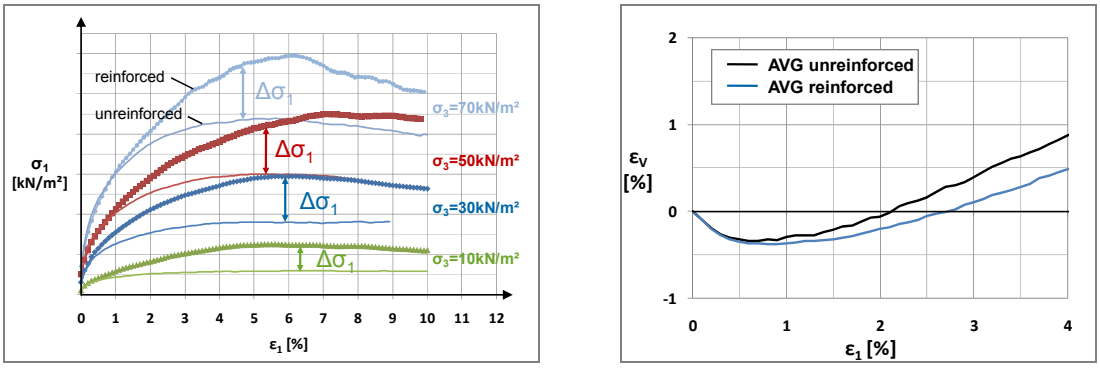

a) Bearing capacity of unreinforced and reinforced samples b) Average volumetric strains

Figure 3. Test results of samples with base course material compacted to 95% D_{pr}.

The distribution of geogrid strains is given for the geogrid placed at mid height (0.55m) at ε_1 = 1% vertical strain in Figure 4. The strains are continuously increasing from the edge towards the center of the sample and correspond directly with the tensile force acting in the geogrid. Maximum strains are situated in the center of the sample, because at this point the maximum anchorage length of 0.25m is provided in each direction. Similar observations were made by Ketchart and Wu (2001) who obtained the strain distribution from laboratory tests as well as from finite element calculations.

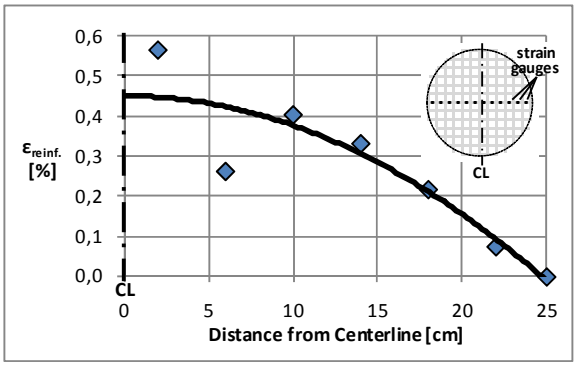

Figure 4. Strain distribution in the geogrid at mid height.

2. MECHANICAL MODEL FOR THE COMPOSITE MATERIAL

The mechanical model shown in Figure 5a has been derived from the large triaxial testing results of the reinforced soil. Caused by the vertical compression during loading the sample extends radially. As stated above, this is accompanied by the activation of the geogrids, due to which the deformations are reduced and the bearing capacity is increased. The mechanisms of load transfer between soil and geogrids are described in Ziegler and Timmers (2004) for example.

With progressive deformation of the sample, the confining forces of the geogrids are increasing. As a simplifying assumption, this can be considered as an equivalent, additional confining pressure $\Delta\sigma_3$ supporting the soil uniformly from the outside (Fig. 5), provided that the vertical spacings between the reinforcement layers are small enough.

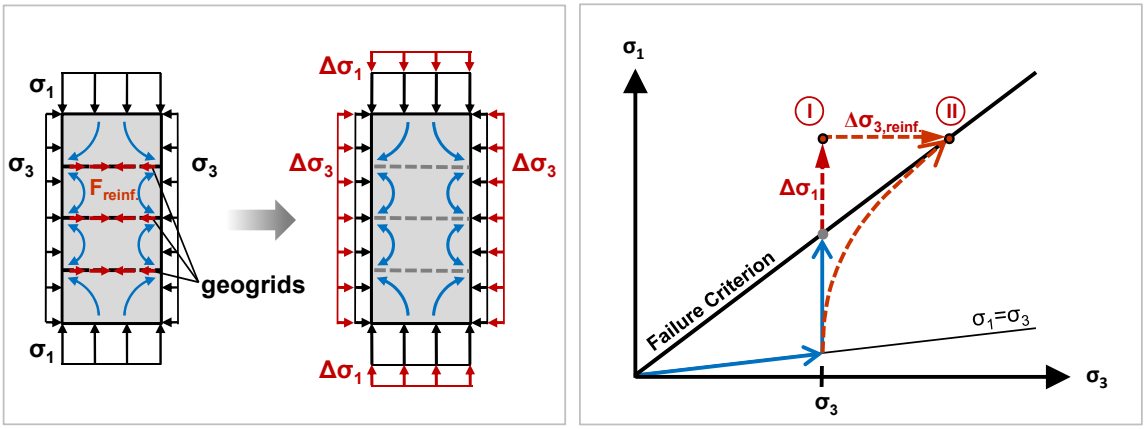

Figure 5. Increased soil strength due to reinforcement (unreinforced: solid line; reinforced: dashed line).

In Figure 5 stress paths of an unreinforced and a reinforced sample are drawn qualitatively. The scale of the axis in the diagram is different in order to show up the details. Therefore, the straight line $\sigma_1 = \sigma_3$, which would normally be the bisecting line is less inclined.

At both tests the samples are being consolidated under hydrostatic conditions before loading. The stress path of the unreinforced sample (continuous line) shows an increase of σ_1 until failure while the cell pressure σ_3 is kept constant. At a reinforced test, an increase of σ_1 beyond the critical limit of the unreinforced soil can be observed, although the cell pressure is the same as it was for the unreinforced test. The obvious, resulting stress condition at failure for "case I" is therefore $\{\sigma_1 + \Delta\sigma_1;\ \sigma_{3,cell}\}$. However, due to the deformation dependant activation of the geogrids and according to the model described above, the effective stress path of a reinforced sample (dashed line) shows actually an increase of the confining pressure by $\Delta\sigma_{3,reinf.}$ during loading. When failure eventually occurs, the stress condition has reached the failure criterion of the unreinforced soil (case II), but at a much higher stress level $\{\sigma_1 + \Delta\sigma_1;\ \sigma_{3,cell} + \Delta\sigma_{3,reinf.}\}$.

Using the method described in Ruiken and Ziegler (2008) the stress paths have been determined also quantitatively for the tests carried out with the reinforced base course material. Although the soil has been consolidated under isotropic conditions ($\sigma_1 = \sigma_3$), in the stress paths shearing off is considered to start from at-rest conditions, because the influence of the self weight can not be neglected for the more than 1 m high sample. The results indicate a benefit of the geogrids for the load bearing capacity at any time during testing.

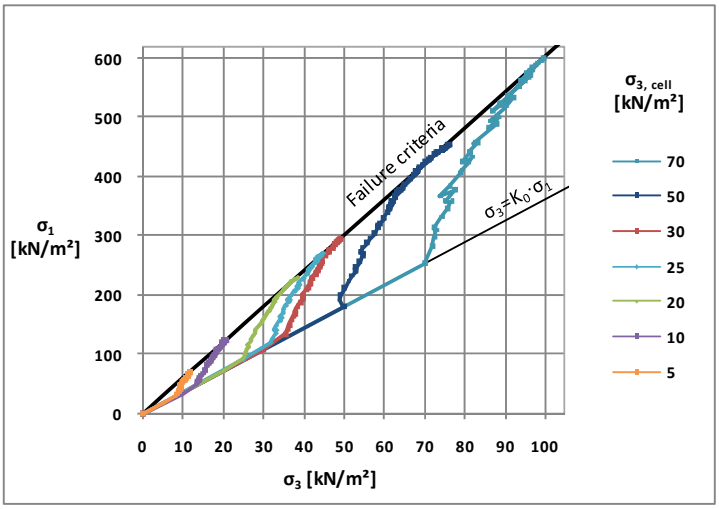

Figure 6. Stress paths for the reinforced base course compacted with 95% D_{pr}.

3. DETERMINATION OF MATERIAL PARAMETERS FOR THE COMPOSITE MATERIAL

Depending on the constitutive law employed in numerical programs to describe the stress-strain behaviour of the soil and the compound material, respectively, different parameters may be required. To carry out calculations using the Mohr-Coulomb model, the knowledge of the friction angle φ and the cohesion c is required to calculate the stability of soil structures in the ultimate limit state. To predict the deformations, further parameters, such as the Young's Modulus E, the Poisson's Ratio ν or the dilatancy angle ψ are required, if linear-elastic stress-strain-behaviour is assumed. This section is dealing with the determination of the shear parameters for the composite material geogrid reinforced soil. The derivation of the last mentioned parameters for the description of the deformation behaviour of the composite material is shown in Ruiken and Ziegler (2009).

3.1 Shear strength of the reinforced soil

In Figure 7a, the results of a series of unreinforced tests as well as those of 20 reinforced tests with base course material compacted to 95% D_{pr} are shown. Results are presented for the conventionally measurable stresses σ_1 and $\sigma_{3,cell}$ at failure (case I, Fig. 5). For the tested unreinforced soil at different stress levels, the failure criterion is a straight line. The plot of σ_1 versus σ_3 can easily be transformed into a τ-σ-diagram with the Mohr-circles, using the Equations [1] and [2] given e.g. by Wittke (1984).

$$\varphi = arcsin\left(\frac{tan\beta - 1}{tan\beta + 1}\right) \quad [1]$$

$$c = b \cdot \left(\frac{1 - sin\varphi}{2\,cos\varphi}\right) \quad [2]$$

The failure criterion obtained for the reinforced tests seems to be parallel to those of the unreinforced soil, which could be described by the same angle of friction and an additional cohesion. However, this cohesion is only of theoretic nature. Results of tests at very low stress levels ($\sigma_3 \leq 20$ kN/m²) indicate that it is not apparent for small lateral pressures. The use of this cohesion in the range of low lateral stresses leads to an over-estimation of the shear strength and, as a consequence, will lead to an over-estimation of the calculated stability of the reinforced soil, Herle and Mašín (2005).

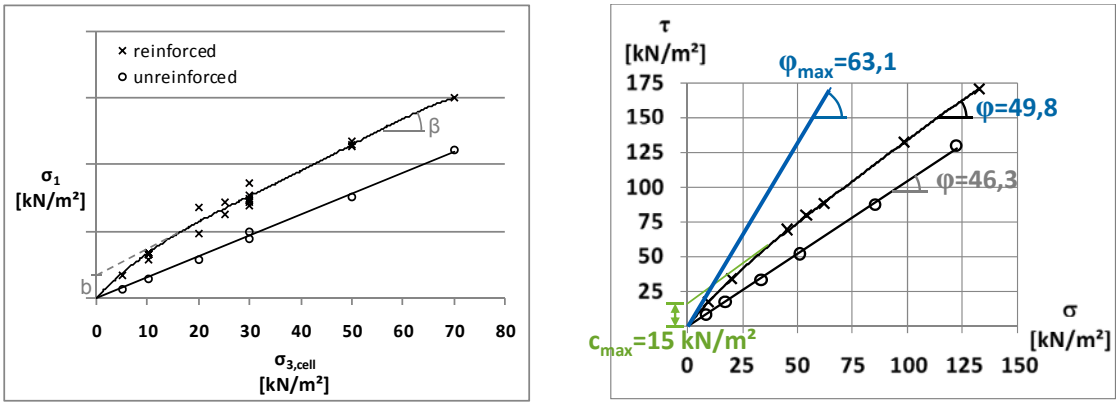

Figure 7 Failure criteria of the unreinforced and reinforced soil (D = 95% D_{pr}).

In Fig. 8 shear parameters are given for both the unreinforced and the reinforced soil for two different degrees of soil compaction, i.e. 95% D_{pr} and 100% D_{pr}. It can clearly be seen, that the non-linear shear parameters do not only depend on the stress level, but also to a considerable degree on the compaction of the soil. A high quality compaction has therefore an elementary meaning to the bearing capacity of the unreinforced as well as of the reinforced soil.

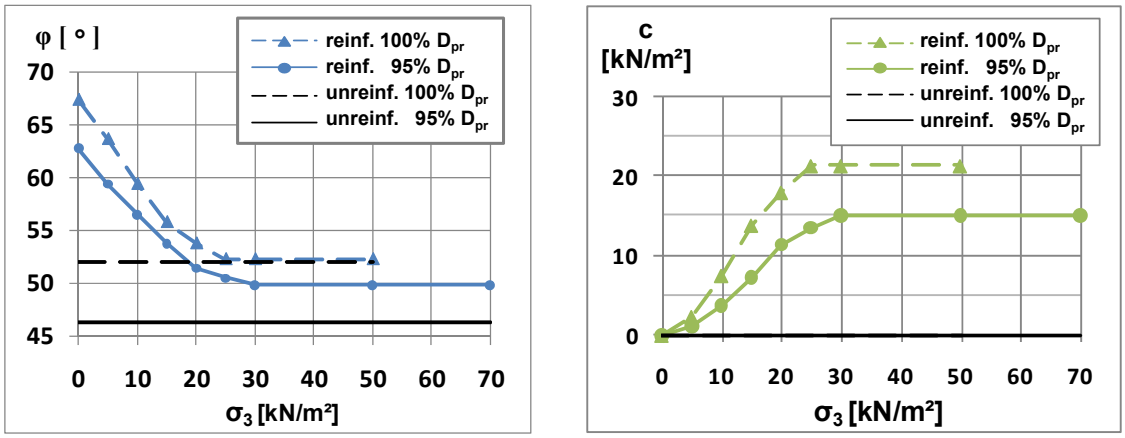

Figure 8. Influence of stress level and degree of compaction on the shear parameters.

Most calculation programs don't provide a possibility of using non-linear shear parameters. With a good approximation, for the tested reinforced soil the failure criterion can be considered to be bilinear (left plot of Fig. 9), being on the safe side. This allows to model the reinforced soil with layer-wise constant shear parameters, as shown in the right plot of Figure 9.

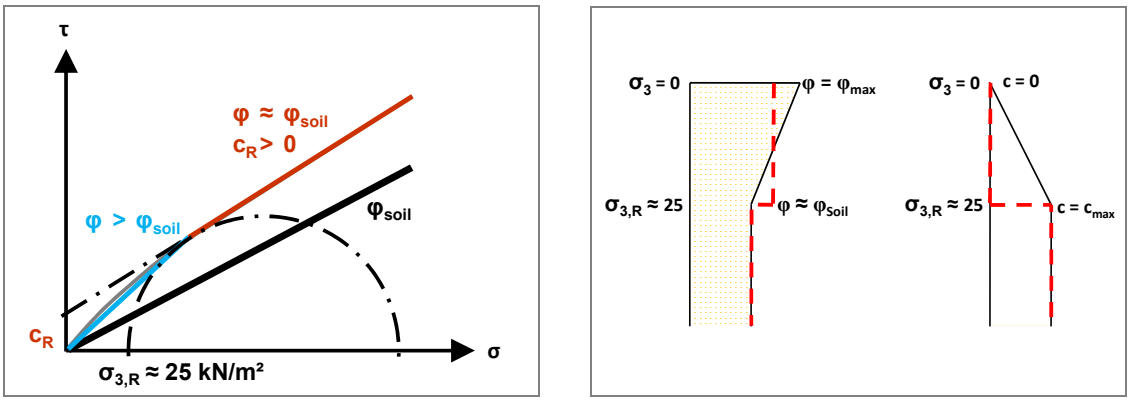

Figure 9. Bilinear failure criterion of the geogrid / soil composite material and simplified approximation.

The shear parameters of the composite material (φ_c and c_c) could be described as below, in dependency of the prevailing stress condition.

$\sigma \leq \sigma_{3,R}$:	$\varphi_c > \varphi_{Soil}$	$c_c = c_{Soil}$	(here: $c_{Soil} = 0$)
$\sigma > \sigma_{3,R}$:	$\varphi_c \approx \varphi_{Soil}$	$c_c > c_{Soil}$	

A similar approach was made by De Buhan et al. (1989), who described reinforced earth as a homogeneous material. To ensure that the reinforcing effect is acting throughout the whole soil body, a limitation of the maximum vertical reinforcement spacing was added.

4. CONCLUSIONS

Reinforced large scale triaxial tests show in comparison with unreinforced tests a significant increase of the bearing capacity and reduction of the deformations due to the geogrids, which is consistent with observations made in field. The confining effect of the geogrids has been identified as responsible for the favourable stress-strain-behaviour of the reinforced soil.

The shear parameters derived for the composite material have shown that the geogrids lead to an increase of the shear strength and the stiffness of the soil. This is consistent for all stress levels tested. Due to the non-linear nature of the shear parameters, it is important to determine the parameters under similar conditions as in-situ.

ACKNOWLEDGEMENTS

The authors would like to thank Naue GmbH & Co. KG for providing the geogrids and for financial support for carrying out the triaxial compression tests.

REFERENCES

De Buhan, P., Mangiavacchi, R., Nova, R., Pellegrini, G., Salençon, J. (1989): Yield design of reinforced earth walls by a homogenization method. *Géotechnique 39*, No. 2, 189-201.

Herle, I., Mašín, D. (2005): Einfluss von bodenmechanischen Aspekten auf numerische Ergebnisse. Tagungsband FEM in der Geotechnik (Qualität, Prüfung, Fallbeispiele), Arbeitsbereich Geotechnik und Baubetrieb, TU Hamburg-Harburg, Heft 10, 53-66.

Ketchart, K. and Wu, J.T.H. (2001). Performance test for geosynthetic reinforced soil including effects of preloading. *Federal Highway Administration*, McLean, VA, USA, Report No. FHWA-R-01-018.

Ruiken, A. and Ziegler, M. (2008). Effect of Reinforcement on the Load Bearing Capacity of Geosynthetic Reinforced Soil. *EuroGeo4*, igs, Edinburgh, UK, (Proceedings in CD).

Ruiken, A. and Ziegler, M. (2009). Ableitung von Systemkennwerten für den Verbundbaustoff Geogitter / Boden aus Triaxialversuchen, *Geokunststoff-Kolloquium der Naue Unternehmensgruppe*, Bad Wildungen, Germany, (Proceedings in print).

Wittke, W. (1984): Felsmechanik: Grundlagen für wirtschaftliches Bauen im Fels. *Springer-Verlag*, Heidelberg.

Ziegler, M., Timmers, V. (2004): A new approach to design geogrid reinforcement. *EuroGeo3*, igs & DGGT, Munich, Germany, Vol. 2, 661-666.